Compressed Sensing Reception of Bursty UWB Impulse Radio is Robust to Narrow-band Interference

Anand Oka and Lutz Lampe
Dept. of Electrical and Computer Eng., University of British Columbia, Canada. {anando, lampe}@ece.ubc.ca

***Abstract*—We have recently proposed a novel receiver for Ultra-Wide-band Impulse-Radio communication in bursty applications like Wireless Sensor Networks. The receiver, based on the principle of Compressed Sensing (CS), exploits the sparsity of the transmitted signal to achieve reliable demodulation. It acquires a modest number of projections of the received signal using analog correlators, and performs a joint decoding of the time of arrival and the data bits from these under-sampled measurements via an efficient quadratic program. In this paper we examine the robustness of this receiver to strong narrow-band interference (NBI) from primary licensed systems like WiMAX. First, by choosing frequency selective test functions in the front-end correlators, we ensure that the interferer can corrupt only a small fraction of the CS measurements. Then we implement a 'digital notch' by identifying and dropping those affected measurements during the quadratic programming reconstruction. The method is easily extended to multiple interferers without additional cost or complexity. We show that by implementing such a 'digital notch' the receiver becomes extremely robust to NBIs. For example its performance is negligibly affected even when the WiMAX customer premise equipment is at a distance comparable to that of the UWB transmitter and the base station is only ten times farther off, both very practical scenarios.**

I. Introduction

On account of its ability to trade bandwidth for a reduced transmit power, Ultra-Wide-band (UWB) Impulse Radio (IR) [1] [2] is a promising candidate for power constrained applications like wireless sensor networks. However, in such applications the traffic is often bursty with a low duty cycle, which implies that there is a large timing uncertainty at the start of each burst, and the usual approach of using long training headers for accurate timing acquisition is unsatisfactory due to an excessive overhead. Secondly, due to the prohibitive complexity of fast A/D conversion and maximum likelihood sequential estimation (MLSE), a commonly used pragmatic approach is to avoid inter-symbol interference (ISI) via a sufficiently low baud-rate, and then use a maximum ratio combining (MRC) rake [3], an energy detector (ED) [4] or a transmit-reference (TR) receiver [5]. Unfortunately, the price paid in doing so is a significantly lowered instantaneous data rate and long channel occupancy.

In light of these issues, in [6] we proposed a novel receiver that performs a 'joint' decoding of timing and amplitude information, by exploiting the *sparsity* (burstiness) of the transmitted signal, thus turning an apparent drawback into a strength. This joint decoding is inspired by the principle of compressed sensing (CS) [7] [8]. The architecture completely bypasses the requirement of high-rate A/D conversion. Instead we use an analog front-end consisting of a bank of correlators with tractable test functions and a low-rate A/D converter. The DSP back-end implements a computationally efficient quadratic program (QP). The receiver can operate with various levels of timing accuracy, ranging from a fraction to many multiples of the pulse width T_{pulse}. As the burst size becomes moderately large, it implicitly acquires timing 'on the fly', which allows us to send bursts *without* training headers. Moreover, it works well even in significant ISI, and we are not restricted to a low baud-rate.

In this paper we will study another critical robustness property of the receiver of [6], namely its insensitivity to narrow-band interference (NBI) from primary licensed systems like WiMAX. Note that a generic UWB receiver needs to be kept 'wide open' in the frequency domain in order to gather all the signal energy, which makes it potentially susceptible to strong narrow-band interference from a variety of licensed and unlicensed sources. In a digital correlator or MLSE receiver the dynamic range of the front-end high-speed A/D converter can be easily saturated by the NBI. Similarly analog receivers like rake, ED and TR also suffer heavily because they have no inherent mechanism to reject the interference energy from their decision statistic. Hence some mechanism to 'notch out' the interferer needs to be implemented *in analog, before the signal enters the receiver.* Since one a-priori does not know the frequency location of the interferer, one must identify it and then tune the notch in real time, which adds to the cost and complexity.

In contrast, we will demonstrate in this paper that the CS receiver of [6] has an inherent robustness to narrow-band interference, thanks to its structural properties. Firstly, the correlator test functions used in the analog front end can be chosen to be *highly frequency selective signals* (rather than pseudo-random noise-like signals as in classical CS), without any significant loss in performance. As a consequence, an NBI can corrupt only a small fraction of all the CS measurements. Secondly, we can implement a 'digital notch' by identifying and dropping the affected measurements during reconstruction, thereby recovering essentially all the performance of the interference-free case. Even multiple interferers are easily handled and require no hardware modifications.

Note that [9] have also considered a similar CS approach to NBI mitigation, although there also exist some significant

differences. Firstly [9] require a low pulsing rate so that ISI is avoided, while our receiver can work at any pulsing rate up to the Nyquist frequency. Secondly they do not address the issue of imperfect timing, while our receiver is very robust to the same. Lastly, they use a random CS measurement matrix and hence need to explicitly identify the NBI sparsity sub-space by taking a Discrete Cosine transform. Our CS ensemble itself implements a Fourier analysis of sorts, due to which the NBI subspace is immediately apparent from the magnitude of the CS measurements.

Outline of the paper: In Section II we present the UWB system model, the interference model and, for the sake of self-sufficiency, the receiver architecture from [6]. In Section III we describe the digital notching mechanism, and then present simulations demonstrating the robustness of the scheme in the exemplary scenario of WiMAX interference. Section IV makes concluding remarks.

Convention: With an abuse of notation, $P(x)$ will denote the density or mass function of a random variable X. $U([a,b])$ will denote a uniform distribution over the interval $[a,b]$ of the real line or of integers, depending on the context. When x is a vector, x^T is the transpose, $\|x\|_2$ the L_2-norm (Euclidean length), $\|x\|_1$ the L_1-norm (largest absolute value), and $\|x\|_0$ the number of non-zero elements. $H(f), \Phi(f)$ etc will denote Fourier transforms of continuous-time finite-energy signals $h(t), \phi(t)$ etc. $h(t) \star \phi(t)$ denotes a convolution of the signals.

II. System Model and Receiver Architecture

A. Transmitter and Channel

Please refer to the signal-path diagram shown in Figure 1. The UWB-IR transmitter consists of a timing block that generates a clock signal at a nominal frequency $f_{baud} = 1/T_{baud}$ and an IR pulse generator. The baud clock provides the timing for the IR pulses within each burst, as well as the timing for the start of each burst after requisite down-sampling to a burst rate f_{burst} bursts per second. A total of K pulses are transmitted in each burst after which the transmitter hibernates till the start of the next burst. At the k-th strobe of the clock within a burst, the IR pulse generator sends on the air a pulse $\phi_U(t)$, amplitude modulated by the bit B^k provided by the payload, drawn equiprobably from the alphabet$\{+1,-1\}$. It is nominally centered at the frequency f_{cU} with a bandwidth Ω_U. Define

$$\phi_U^l(t) \doteq \sum_{k=0}^{K-1} b_l^k \phi_U(t - kT_{baud}), \tag{1}$$

$$\theta(f) \doteq \frac{1}{2^K} \sum_{l=0}^{2^K-1} |\Phi_U^l(f)|^2, \tag{2}$$

where $b_l^k \in \{+1,-1\}$ is the k-th bit of the number $l \in \{0,1,\ldots,2^K-1\}$. Then the power spectral density (PSD) of the transmitted bursty UWB signal is given by [10]

$$PSD_U^{TX}(f) = \frac{\theta(f)}{T_{burst}}. \tag{3}$$

Let L_U^{TX} be the *maximum* equivalent isotropically radiated power spectral density (EIRP-SD) allowed under government regulations, and let us assume that $\max_f PSD_U^{TX}(f) = L_U^{TX}$. The UWB channel $c_U(t)$ is known to be linear dispersive with tens or hundreds of resolved multi-path components, and a temporal dispersion as large as 100 nanoseconds in indoor environments [11]. Additionally, there is a path-loss (spreading loss) of $d_U^{-\rho}$, where d_U be the distance of the UWB transmitter from the UWB receiver, and ρ is the path-loss exponent.

For example, consider the Hanning modulated RF pulse of [2] which we used in our simulations, with $f_c = 4.0$ GHz and a 6-dB bandwidth $\Omega_U = 2.0$ GHz. The pulse duration is small, $T_{pulse} = 1.0$ nanosecond. Since our receiver can tolerate significant ISI, we may choose a baud-rate close to the Nyquist frequency, say $f_{baud} = f_{nyquist}/8 = 500$ Mbaud. Hence the interval between consecutive pulses is $T_{baud} \doteq 1/f_{baud} = 2.0$ nanoseconds, and a burst of $K = 64$ bits (say) will last for 127 nanoseconds. In contrast, the interval between consecutive bursts may be as large as $T_{burst} = 1/f_{burst} = 100$ microseconds. A practical inexpensive clock has a timing drift of $\varrho \sim 40$ parts per million (p.p.m.) caused by random frequency modulation [12]. While the total drift from the beginning to the end of a burst is limited to a negligible value of $K\varrho f_{baud} = 5.1$ picoseconds, the drift from one burst to the the next is ~ 4.0 nanoseconds, which is relatively very large. Even with a coarse timing algorithm for predicting the start of the bursts, like a second-order tracking loop, a residual tracking error of the order of 1.0 nanosecond is unavoidable.

Without loss of generality we can concentrate on the reception of a single burst, and treat the estimated time of arrival (TOA) of that burst as the temporal origin $t = 0$. The residual error of the coarse timing block is then perceived as a late arrival of the actual burst by an amount υ seconds. (By prefixing a sufficient guard interval in the coarse timing estimate, we can ensure that the true arrival can only be late but never early.) For simplicity suppose that the true TOA υ is distributed over the interval $[0,\gamma]$ according to a uniform density. From the point of view of the receiver, the output of the transmitter during the burst is then written as

$$S(t) = \sum_{k=0}^{K-1} B^k \, \phi(t - kT_{baud} - \upsilon). \tag{4}$$

Notice that in writing this equation we ignore the small timing drift within a burst.

B. Interference Model

Suppose there is a narrow-band interferer (NBI) at a distance d_I from the UWB receiver. Let the pulse shape used by the NBI be $\phi_I(t)$, nominally centered at f_{cI} and having a bandwidth $\Omega_I \ll \Omega_U$, and let its signalling interval be T_I. Then, assuming that the NBI uses a zero-mean unit-power signalling constellation, its EIRP is given by

$$P_I^{TX} = \frac{\int |\Phi_I(f)|^2 df}{T_I}. \tag{5}$$

The interferer sees a channel $c_I(t)$ to the UWB receiver, and a path-loss of $d_I^{-\rho}$.

C. SNR and SIR in an Optimal Matched Filter Receiver

Let $h_U(t) \doteq \phi_U(t) \star c_U(t)$, and analogous to equations (1),(2) define

$$h_U^l(t) \doteq \sum_{k=0}^{K-1} b_l^k h_U(t - kT_{baud}), \quad (6)$$

$$\xi(f) \doteq \frac{1}{2^K} \sum_{l=0}^{2^K-1} |H_U^l(f)|^2. \quad (7)$$

An optimal (but intractable) receiver would replace the front-end filter $g(t)$ with a bank of 2^K matched filters (MFs), one each for the candidate signal $h_U^l(-t), l = 0, 1, \ldots, 2^K - 1$. Assuming that the *timing is perfectly known*, it would then declare as the estimate of the payload the index l of the filter which has the maximum output at the sampling time. Such a hypothetical genie-timed MF receiver serves as a reference with which we can compare our suboptimal receiver. The average signal to noise ratio (SNR) per bit in the MF receiver is given by

$$\text{SNR}_{bit} \doteq \frac{d_U^{-\rho} \int \xi(f) df}{K \frac{N_0}{2}}, \quad (8)$$

where $\frac{N_0}{2}$ is the two-sided power spectral density of the zero-mean additive white Gaussian (AWG) thermal noise $V(t)$. Similarly define $h_I(t) \doteq \phi_I(t)$, and

$$h_{cross}^l(t) \doteq h_I(t) \star h_U^l(-t), \quad (9)$$

$$\chi(f) \doteq \frac{1}{2^K} \sum_{l=0}^{2^K-1} |H_{cross}^l(f)|^2. \quad (10)$$

Then the average signal to interference ratio (SIR) per bit is given by

$$\text{SIR}_{bit} = \left(\frac{d_I}{d_U}\right)^{\rho} \frac{T_I \left(\int \xi(f) df\right)^2}{K \int \chi(f) df}. \quad (11)$$

Note that the SIR so defined is additively compatible with the SNR in the mean squared error sense. That is, the net signal to perturbation ratio (SPR) per bit in the MF receiver is

$$\text{SPR}_{bit} = \frac{1}{\frac{1}{\text{SNR}_{bit}} + \frac{1}{\text{SIR}_{bit}}}. \quad (12)$$

D. Receiver

The tractable suboptimal receiver proposed in [6] consists of an analog front-end and a DSP back-end. Its defining characteristic is that it relieves the analog front-end of difficult tasks like fast A/D conversion and accurate delay lines, and instead compensates by using an elaborate but tractable DSP back-end.

1) Analog Front-end: The first block in the analog front-end is a noise-limiting bandpass-pass filter $g(\cdot)$ centered at f_c and having a bandwidth $\approx \Omega_U$. Its output is

$$R(t) = \sum_{k=0}^{K-1} B^k h(t - kT_{baud} - \upsilon) + W(t) + I(t), \quad (13)$$

where the three terms are, respectively, the UWB signal, thermal noise and the interference signal. Here $h(t) \doteq \phi_U(t) \star c_U(t) \star g(t)$ is the total impulse response seen by the UWB transmitter. $W(t) = \int V(t-\tau) g(\tau) d\tau$ is the band-limited response of the filter $g(\tau)$ to the thermal noise process $V(t)$, and $I(t)$ is its response to the incoming interference signal.

Let λ_h denote the length of the total impulse response $h(t)$. The signal $R(t)$ is fed to a bank of M parallel analog correlators, followed by M integrators. The test function used in correlator number m is denoted as $\psi_m(t)$, and the whole ensemble of test functions is denoted by $\{\psi_m(t)\}$, which is assumed to be known to the DSP back-end. In Section III-A we will discuss the criteria for selecting the ensemble. The integrators $m = 0, 1, \ldots, M-1$ are reset to zero at the epoch $t = 0$ and their output is sampled synchronously at the epoch $\lambda_h + \gamma + (K-1)T_{baud}$ when all of the energy of the burst is known to have arrived with high probability. Thus, for $m = 0, 1, \ldots, M-1$, we have the M *measurements*

$$Y_m = \int_0^{\lambda_h + \gamma + (K-1)T_{baud}} R(t) \psi_m(t)\, dt. \quad (14)$$

The vector of measurements $Y = [Y_0, Y_1, \ldots, Y_{M-1}]^T$ is then fed to the DSP back-end, which recovers the payload bits $B^k,\ k = 0, 1 \ldots, K-1$ via a tractable QP algorithm.

2) DSP Back-end: The demodulation of the payload by the DSP back-end relies on a consistent discrete time representation of the signal. Let f_s be a sufficiently large *virtual sampling frequency* [13] for the received UWB-IR signal. We would like to emphasize that this is only a 'thought-experiment' construction, and no A/D conversion is done at rate f_s in actuality. Let $T_s \doteq 1/f_s$, and define $h[n] \doteq h(nT_s),\ n = 0, 1, \ldots, \Lambda_h - 1$ and $h \doteq [h[0], h[1], \ldots, h[\Lambda_h - 1]^T$, where $\Lambda_h = \lceil \lambda_h f_s \rceil$ is the length of the discrete-time finite impulse response $h[n]$. A similar convention will apply to other signals like $g(t), \psi_m(t), W(t)$ etc. Let γ and T_{baud} be multiples of T_s, which can be achieved by construction. Now, expressed in rate f_s samples, the TOA uncertainty is $\Gamma \doteq \gamma f_s$ and the baud period (the interval between consecutive pulses) is $N_{baud} = T_{baud} f_s$. Define $\Lambda_X \doteq \Gamma + (K-1)N_{baud}$. Then the length of the total burst response including the timing uncertainty is $N \doteq \Lambda_h + \Lambda_X - 1$.

Let $\Upsilon = \text{round}(\upsilon f_s)$ be the burst TOA υ quantized to a step size of T_s. The quantization error can be made negligible provided f_s is chosen large enough. Now, the sampled version of $R(t)$ can be written as a vector $R \in \mathbb{R}^N$ given by

$$R = \mathcal{H} X + W + I. \quad (15)$$

Here the vector $X \in \mathbb{R}^{\Lambda_X}$ is a *virtual* discrete time information signal which has all samples equal to zero except for K non-zero samples. The k-th non-zero sample, for $k = 0, 1, \ldots, K-1$, has a random amplitude B^k drawn independently and equiprobably from $\{-1, +1\}$, and has a random location $\Lambda^k = \Upsilon + kN_{baud}$. On account of the modeling assumption made in Section II-A, it follows that $\Upsilon \sim U([0, \Gamma])$. The vectors $W, I \in \mathbb{R}^N$ are the sampled version of the additive Gaussian noise $W(t)$ and interference $I(t)$ respectively, and the matrix $\mathcal{H} \in \mathbb{R}^{N \times \Lambda_X}$ is the convolutional matrix (Toeplitz form) of $h[n]$ [14]. In a similar vein we can further relate the actually sampled measurements Y at

the output of the integrators to the virtual information signal X. Define the $M \times N$ *measurement matrix*

$$\Psi \doteq \frac{1}{f_s}\Big[\psi_0, \psi_1, \dots \psi_{M-1}\Big]^T, \tag{16}$$

where $\psi_i \doteq \Big[\psi_i[0], \psi_i[1], \dots, \psi_i[N-1]\Big]^T$, $\forall i = 0, 1, \dots, M-1$. Then we can write the *measurement equation*

$$Y = \Psi R = \Psi \mathcal{H} X + \Psi W + \Psi I. \tag{17}$$

Let $B \doteq [B^0, B^1, \dots, B^{K-1}]^T$. The aim of the DSP back-end is to optimally estimate B, Υ from the measurement Y, based on the relation in equation (17) and the a-priori statistical knowledge about B, Υ. Note that B contains the payload which is of primary interest, while the quantity Υ is a 'nuisance' parameter. We assume that the system response $h(t)$ is known to the receiver, up to a random TOA υ. This can be achieved by a tandem identification algorithm [6].

E. Bit Demodulation Based on Incomplete Measurements

Let us define the set $\mathcal{X}$ as the set of all signals $x \in \mathbb{R}^{\Lambda_X}$ that satisfy the following properties:

1) $\|x\|_0 = K$ (sparsity).
2) The first nonzero sample is located at $\ell^0 \in [0, \Gamma]$. The subsequent non-zero samples are located at positions $\ell^k = \ell^0 + kN_{baud}$, $\forall k = 1, 2, \dots, K-1$ (timing).
3) The magnitudes of all the nonzero samples are from $\{-1, +1\}$ (signaling alphabet).

Clearly $|\mathcal{X}| = 2^K(\Gamma+1)$, $\mathcal{X}$ is the finite equiprobable alphabet of the random information signal X (cf. Section II-D2), and there is a one-to-one mapping

$$\{-1, +1\}^K \times \{0, 1, \dots, \Gamma\} \rightarrow \mathcal{X} \tag{18}$$

$$(B, \Upsilon) \mapsto X(B, \Upsilon). \tag{19}$$

Hence we can write $P(Y|B, \Upsilon) = P(Y|X)$, which implies that, without losing optimality, we may first make the ML estimate $\hat{X}$ of the information signal X, and then map it to the optimal estimates of the payload $\hat{B}(\hat{X})$ and TOA $\hat{\Upsilon}(\hat{X})$. It is straightforward to show that *if we ignore the interference term* ΨI in equation (17) (whose statistics are a-priori unknown to us) and consider only the additive Gaussian noise, the ML demodulator declares the estimated signal as [6]

$$\hat{X} = \underset{x \in \mathcal{X}}{\operatorname{argmin}} \ (Y - \Psi\mathcal{H}x)^T(\Psi\mathcal{G}\mathcal{G}^T\Psi^T)^{-1}(Y - \Psi\mathcal{H}x), \tag{20}$$

where $\mathcal{G}$ is the Toeplitz matrix of $g(t)$. Unfortunately, the complexity of the ML demodulation problem (20) scales as $2^{\min(K, \lambda_h f_{baud})}$), which is clearly impractical. Hence in [6] we proposed an alternative suboptimal demodulation technique whose complexity is $O(K^3)$. Let the vector $\xi(a, \ell_1, \ell_2)$ be a positive penalty vector for the candidate information signals $x \in \mathcal{X}$. It incorporates the available timing information by giving more penalty to those locations of x where the occurrence of the non-zero samples is unlikely. That is, for all $n = 0, 1, \dots, \Lambda_X - 1$,

$$\xi(a, \ell_1, \ell_2)[n] \doteq \begin{cases} & n = \ell + kN_{baud} \\ 1.0, & \ell \in [a + \ell_1, a + \ell_2] \\ & k \in \{0, 1, \dots, K-1\} \\ \mho, & \text{otherwise,} \end{cases} \tag{21}$$

where $\mho$ is some suitable large number like 10^3. Also define a corresponding diagonal penalty matrix as $\Xi(a, \ell_1, \ell_2) = diag(\xi(a, \ell_1, \ell_2))$. Now consider the following relaxation of the ML demodulation problem of equation (20):

$$\tilde{X} = \underset{x \in \mathbb{R}^N \| \Xi(a, \ell_1, \ell_2)\, x\|_1 = K}{\operatorname{argmin}} (Y - \Psi\mathcal{H}x)^T(\Psi\mathcal{G}\mathcal{G}^T\Psi^T)^{-1}(Y - \Psi\mathcal{H}x). \tag{22}$$

Notice that the new constraint set is not discrete, but rather a continuous set of signals of adequately small L_1 norm. Therefore notice that $\mathcal{X} \subset \{x \in \mathbb{R}^N : \|\Xi(0, 0, \Gamma)\, x\|_1 = K\}$. With some manipulation we can re-write (22) as [7]

$$\begin{aligned} \tilde{X}_n &= \tilde{Z}_n - \tilde{Z}_{n+N}, \ n = 0, 1, 2, \dots, N, \\ \tilde{Z} &= \min f^T z + \tfrac{1}{2} z^T Q z \\ & \quad z \geq 0, \ [\xi(a, \ell_1, \ell_2)^T, \xi(a, \ell_1, \ell_2)^T] z = K, \end{aligned} \tag{23}$$

$$Q = \begin{pmatrix} \mathcal{H}^T\Psi^T(\Psi\mathcal{G}\mathcal{G}^T\Psi^T)^{-1}\Psi\mathcal{H} & -\mathcal{H}^T\Psi^T(\Psi\mathcal{G}\mathcal{G}^T\Psi^T)^{-1}\Psi\mathcal{H} \\ -\mathcal{H}^T\Psi^T(\Psi\mathcal{G}\mathcal{G}^T\Psi^T)^{-1}\Psi\mathcal{H} & \mathcal{H}^T\Psi^T(\Psi\mathcal{G}\mathcal{G}^T\Psi^T)^{-1}\Psi\mathcal{H} \end{pmatrix}, \tag{24}$$

$$f = [-Y^T(\Psi\mathcal{G}\mathcal{G}^T\Psi^T)^{-1}\Psi\mathcal{H}, Y^T(\Psi\mathcal{G}\mathcal{G}^T\Psi^T)^{-1}\Psi\mathcal{H}]. \tag{25}$$

(23) is now a standard QP, which has several efficient large-scale techniques of solution, of which $O(K^3)$ interior point methods are generally the fastest [15]. We perform the demodulation in two stages. In the first stage we solve the QP in (23) using $\xi(a = 0, \ell_1 = 0, \ell_2 = \Gamma)$. The result of this stage, $\tilde{X}^{(1)}$, is used to extract an estimate $\hat{\Upsilon}$ of the arrival time via correlation with the template $\xi(0, 0, 0)[n]$ as follows:

$$\hat{\Upsilon} = \underset{n' \in \{0, 1, \dots, \Gamma\}}{\operatorname{argmax}} \sum_n |\tilde{X}^{(1)}[n - n']| \ \xi(0, 0, 0)[n]. \tag{26}$$

We then solve the QP in (23) again, using $\xi(a = \hat{\Upsilon}, \ell_1 = 0, \ell_2 = 0)$. From the result $\tilde{X}^{(2)}$, we demodulate the payload

$$\hat{B}^k = sign(\tilde{X}^{(2)}[\hat{\Upsilon} + k\, N_{baud}]), \ k = 0, 1, \dots, K-1. \tag{27}$$

We would like to point out that the performance of the (ML or QP) demodulator is *invariant* w.r.t. the burst length K even when the number of correlators M is held *constant*.

III. Robustness to Narrow-band Interference

A. Choice of Measurement Ensemble

It was shown in [7], [8] that $\{\psi_m(t)\}$ can be any universally *decoherent* measurement ensemble of randomly generated noise-like signals. However, we actually do not need such universality since we known that our signal sparsity is always in the temporal domain [16]. Hence the *Fourier* ensemble of *sinusoids* of amplitude $1/\sqrt{N}$ and frequencies selected *deterministically and uniformly* from the signal band $[f_c - \frac{\Omega}{2}, f_c + \frac{\Omega}{2}]$ is optimally decoherent w.r.t. the UWB signal. In fact such an ensemble is highly desirable when we face strong NBI because the two are mutually *coherent*. As a consequence the NBI can affect only a few CS measurements. In contrast, no matter which M test functions we choose we are likely to capture roughly a fraction $\frac{Mf_s}{2\Omega N}$ of the received UWB signal's energy. This implies that reliable demodulation of the UWB-IR signal is possible after paying an under-sampling penalty of roughly $10 \log_{10} \frac{2\Omega N}{Mf_s}$ dB, and this penalty will (on an average) decrease monotonically and vanish as $M \uparrow N\frac{2\Omega}{f_s}$.

B. Digital Notch

As we indicated above, if we choose an appropriate measurement ensemble that is coherent w.r.t. the NBI but decoherent w.r.t. the UWB signal, it is assured that the NBI can corrupt only a few CS measurements and we can therefore implement a *digital notch* to suppress those measurements. This is achieved as follows. Suppose for the time being that there can be at the most $n_I = 1$ NBI. Let

$$\hat{m} = \underset{m\in\{0,1,..,M-1\}}{\operatorname{argmax}} |Y_m|. \tag{28}$$

Now let D be an even number and

$$Y_{notched} = [Y_0, Y_1, \ldots, Y_{\hat{m}-\frac{D}{2}}, Y_{\hat{m}+\frac{D}{2}}, \ldots, Y_{M-2}, Y_{M-1}]^T \tag{29}$$

be a shortened vector obtained by notching out the $D+1$ measurements around the index $\hat{m}$. Now we simply execute the QP demodulation in equations (23),(24),(25) using $Y_{notched} \in \mathbb{R}^{N-D-1}$ in lieu of $Y \in \mathbb{R}^N$, along with the appropriate corresponding sub-matrix of Ψ. D can be chosen quite small, say $D \sim \beta\frac{\Omega_I}{\Delta}$, where $\Delta = \frac{\Omega_U}{M}$ is the frequency spacing of the test functions and β is a safety factor to account for leakage into adjacent measurements. We found that $\beta \sim 4-8$ works well. Note that a smaller β can be used if we choose test functions with better frequency selectivity. Finally, if $n_I > 1$ interferers are expected, we simply apply the above notching procedure around the n_I largest absolute values in Y.

Our simulations presented in Section III-C indicate that whenever the NBI are of any significant strength (say $\text{SIR}_{bit} \leq$ 20 dB), they can be very reliably detected and notched by the above method. If an interferer is very weak we may mis-detect and hence fail to suppress it. This, by itself, will have no noticeable impact (since it is weak). But will the unintended side-effect of notching out valid (uncorrupted) measurements be catastrophic? The decoherence property of the CS ensemble ensures that this is not the case. In fact, since each CS measurement on an average captures an equal fraction of the UWB signal energy, in the *interference-free regime* the performance penalty due to the notching of $(D+1)$ CS measurements, w.r.t. an un-notched matched filter receiver, is limited to a maximum of

$$-10\log_{10}\left(1-\frac{n_I(D+1)}{M}\right) \sim -10\log_{10}\left(1-\frac{n_I\beta\Omega_I}{\Omega_U}\right) \text{ dB}. \tag{30}$$

Of course, when strong NBIs are actually present, the digitally notched CS-QP receiver does *not* have any extra perfromance loss while the un-notched matched filter can be completely disabled. Thus the performance penalty in equation (30) is a cost we pay 'up-front' to achieve robustness against n_I interferers, whatever their actual strength (within reason). For example, if we plan for $n_I = 2$ WiMAX NBIs of bandwidth $\Omega_I = 20$ MHz, the performance penalty is only 0.75 dB, which is a very modest.

Finally, another variant is possible where, instead of deciding a-priori on the number of possible NBIs we wish to be immune against (n_I), we choose it on a burst-to-burst basis. That is, in each burst we notch out the n_I CS measurements *whose absolute value crosses a certain pre-defined threshold.* Thus n_I is now a random variable. Therefore, we can in effect adapt the notching to the number of NBIs actually active. Note that we must set the threshold conservatively (i.e. not too high) so that we reliably detect and notch the NBIs when they are present. This means we will suffer some 'false alarms' and intermittently notch uncorrupted measurements. Hence, instead of a fixed deterministic penalty, we pay a 'stochastic' penalty for achieving NBI robustness, and its average value will be given by the expectation of equation (30) w.r.t. the distribution of n_I conditioned on an interference-free regime.

C. Simulations of WiMAX Interference

As an exemplary case we simulate interference from a WiMAX transmitter (IEEE 802.16-2004 [17] and later). We consider the maximum allowed bandwidth under the draft standard, namely $\Omega_I = 20$ MHz, which constitutes the worst case from the point of view of the UWB system. We choose a center frequency of $f_{cI} = 4.0$ GHz (out of the possible range $2-66$ GHz), since it falls approximately in the middle of our UWB spectrum (cf. Section II-A). We simulate the presence of WiMAX customer premise equipment (CPE) (uplink) with a standard transmit power $P_I^{TX} \sim 23$ dBm. From these results the performance in the presence of a base station (BS) (downlink) having $P_I^{TX} \sim 43$ dBm can be easily inferred, as we shall see shortly. For the UWB transmitter we choose the FCC specified PSD limit $L_U^{TX} = -41.3$ dBm/MHz [12].

We randomly generate two channel realizations from the CM1 model of [11], normalize them to unit energy (since we model the distance-based path loss separately) and specify them as the responses $c_U(t), c_I(t)$, which are held constant throughout. Note that the temporal dispersion of the CM1 channel can be as large as 50 to 100 nanoseconds. We set $g_U(t)$ to be a Nyquist filter of bandwidth Ω_U around f_{cU}, adequately delayed and truncated in time for realizability. All simulations are performed with $f_s = 10$ GHz, $K = 8$ bits per burst, $\rho = 2.0$, $f_{baud} = 500$ Mbaud (implying that ISI extends for $25-50$ pulses), $f_{burst} = 1$ Mbursts per second, and $T_I = \frac{1.5}{2\Omega_I} = 37.5$ nanoseconds (hence a 50% roll-off in the WiMAX modulation). We use the IR pulse described in Section II-A and the CS-QP demodulation described in Section II-D2. A Fourier ensemble is used, as described in Section III-A, with the M test functions located uniformly from 2.5 to 5 GHz. (An asymmetric range is chosen around the center frequency $f_c = 4.0$ GHz to exploit the 'tilt' in the channel frequency response.) A Tuckey window is applied to each test function to ensure sufficiently rapid decay of its spectrum away from its center frequency, in order to minimize leakage. In the following discussion, the quantity $\frac{Mf_s}{2\alpha\Omega N}$, with $\alpha = 1.5$, will be called the *under-sampling factor*, such that $\frac{Mf_s}{2\alpha\Omega N} = 1$ implies adequate sampling while $\frac{Mf_s}{2\alpha\Omega N} < 1$ implies under-sampling.[1]

Figure 2(a) shows the PSD of the UWB and the NBI signals at the input of the filter $g(t)$ under the condition $\text{SIR}_{bit} =$

[1]For a strictly band-limited $\phi_U(t)$, $\alpha = 1.0$. For the practical pulse we use, we empirically determined that $\alpha = 1.5$ ensures a performance indistinguishable from Nyquist rate time-domain sampling.

25 dB, as well as the spectra of a couple of exemplary test functions. Figures 2(b),(c) show the contribution of the UWB signal and the WiMAX NBI to the CS measurements when $\frac{Mf_s}{2\alpha\Omega N} = 1.0$. Subplot (a) shows the case when the NBI is co-located with a test function and (b) shows the case when it falls in inbetween two adjacent test functions. It is clear that even for such relatively high SIR, the NBI stands out in magnitude in both cases and can be reliably detected. Note that if we operate with significant undersampling $\frac{Mf_s}{2\alpha\Omega N} \ll 1.0$, the test functions are not densely packed and the NBI can fall 'in between the cracks'. This missed detection is not a problem however since in such a case the NBI will not affect the performance at all. In other words, whenever the NBI is in a position to degrade the receiver performance, we can also reliably detect and digitally notch it.

Next we consider the performance of the digitally notched CS-QP receiver when there is a single NBI colocated with a test function, at various values of SIR_{bit}. We use a fixed value of $n_I = 1$ for the digital notch. Note that a given value of SIR_{bit} translates to a unique value of $\frac{d_I}{d_U}$ according to equation (11). Some exemplary values of this relationship are provided in Table I for the case of a WiMAX CPE as well as BS. We simulate four cases, namely (i) Adequate sampling and perfect timing: $\frac{Mf_s}{2\alpha\Omega N} = 1.0$, $\gamma = 0$, (ii) Under-sampling and perfect timing: $\frac{Mf_s}{2\alpha\Omega N} = 0.25$, $\gamma = 0$, (iii) Adequate sampling and poor timing: $\frac{Mf_s}{2\alpha\Omega N} = 1.0$, $\gamma = 1.0$ nanosecond, and (iv) Under-sampling and poor timing: $\frac{Mf_s}{2\alpha\Omega N} = 0.25$, $\gamma = 1.0$ nanosecond. We present the results in the four respective sub-plots of Figure 3. In subplot Figure 3(a) for reference we also show the performance of the matched filter receiver with perfect timing (cf. II-C) but no interference rejection mechanism. The figure allows us to make several interesting observations.

Firstly, with perfect timing and adequate sampling (subplot (a)) we see that the digitally notched CS-QP receiver is 20 dB more robust to NBI than the un-notched matched filter. Specifically, an SIR_{bit} of 0 dB causes a loss of ~ 0.5 dB at BER 10^{-3} operating point, while for the matched filter an SIR_{bit} of 20 is needed for similar performance. From Table I we know that $\text{SIR}_{bit} = 0$ dB when $d_I/d_U \sim 0.9(9.9)$ for a WiMAX CPE (BS). This implies that the CPE can be as a distance comparable to that of the UWB transmitter, and the BS interferer need be only about ten times further away, to ensure that there is no noticeable impact on the digitally notched CS-QP UWB receiver. This is not an unreasonable scenario. In contrast, a generic un-notched UWB receiver will need the distances to be ten times larger, which essentially means that it cannot co-exist with the WiMAX system. Note that ultimately the CS-QP receiver degrades because of NBI leakage into adjacent CS measurements.

Secondly, we see that the robustness of the digitally notched CS-QP receiver to the NBI is also carried over to the cases of under sampling, imperfect timing or both. We observe, as was expected, that imperfect timing has little effect on performance, since with $K = 8$ the receiver can already acquire timing 'on the fly'. Similarly we verify that the degradation due to under-sampling is graceful and in proportion to the under-sampling factor. That is, $\frac{Mf_s}{2\alpha\Omega N} = 0.25$ leads to around 6 dB loss. In fact, we note that the NBI robustness *improves* when we have under-sampling. This is explained by the fact that with more frequency separation among the test-functions, the NBI leakage into adjacent measurements is further reduced. Finally, we also see that the loss due to under-sampling and imperfect timing is decoupled, i.e. combines additively in dB. In summary, we have verified that all the observations made in [6] for the interference-free case also hold for the scenario of strong NBI.

IV. Concluding Remarks

We have shown that the CS-QP UWB-IR receiver proposed in [6] can be made extremely robust to narrow-band interference by the simple expedient of (a) using frequency selective test functions in the correlators, and (b) implementing a simple digital notching mechanism wherein we identify and drop the few NBI corrputed measurements. For the exemplary case of WiMAX interference, we showed that the receiver remains practically unaffected even when the CPE is at a distance comparable to that of the UWB transmitter and the BS is only ten times farther off.

References

[1] M.Z. Win and R.A. Scholtz. Impulse Radio: How It Works. *IEEE Commun. Letters*, 2(2):36–38, February 1998.

[2] S. Roy, J.R. Foerster, V.S. Somayazulu, and D.G. Leeper. Ultrawideband Radio Design: The Promise of High-Speed, Short-Range Wireless Connectivity. *Proc. of the IEEE*, 92(2):295–311, February 2004.

[3] H. Arslan, Z. N. Chen, and M Di Benedetto. *Ultra Wideband Wireless Communication*. John Wiley & Sons, Inc., 2006.

[4] A. A. D'Amico, U. Mengali, and E. Arias de Reyna. Energy-Detection UWB Receivers with Multiple Energy Measurements. *IEEE Trans. Wireless Commun.*, 6(7):2652–2659, July 2007.

[5] Yi-Ling Chao and R. A. Scholtz. Ultra-wideband transmitted reference systems. *IEEE Trans. Veh. Technol.*, 54(5):1556–1569, September 2005.

[6] Anand Oka and Lutz Lampe. A Compressed Sensing Receiver for UWB Impulse Radio Communication in Wireless Sensor Networks. Submitted to the Elsevier - Physical Communications (Special Issue on Advances in Ultra-Wideband Wireless Communication). Preprint available at www.ece.ubc.ca/∼anando/.

[7] D. L. Donoho. Compressed Sensing. *IEEE Trans. Inform. Theory*, 52(4):1289–1306, April 2006.

[8] E. J. Candes and T. Tao. Near-Optimal Signal Recovery From Random Projections: Universal Encoding Strategies? *IEEE Trans. Inform. Theory*, 52(12):5406–5425, December 2006.

[9] Z. Wang, G. R. Arce, B. M. Sadler, J. L. Paredes, S. Hoyos, and Z. Yu. Compressed UWB Signal Detection with Narrowband Interference Mitigation. *IEEE Int. Conf. on UWB*, 2:157–160, September 2008.

[10] J. Romme and L. Piazzo. On the Power Spectral Density of Time-Hopping Impulse Radio. *IEEE Conference on Ultra Wideband Systems and Technologies*, pages 241–244, 2002.

[11] A. F. Molisch, D. Cassioli, C. C. Chong, S. Emami, A. Fort, B. Kannan, J. Karedal, J. Kunisch, H. G. Schantz, K. Siwiak, and M. Z. Win. A Comprehensive Standardized Model for Ultrawideband Propagation Channels. *IEEE Trans. on Antennas and Propagation*, 54(11):3151–3166, November 2006.

[12] IEEE 802.15.4a-2007. Part 15.4: Wireless Medium Access Control (MAC) and Physical Layer (PHY) Specifications for Low-Rate Wireless Personal Area Networks (WPANs); Amendment 1: Add Alternate PHYs, March 2007.

SIR_{bit} dB	20	10	0	-10	-20
$\frac{d_I}{d_U}$ (WiMAX CPE)	9.9	3.1	0.9	0.3	0.09
$\frac{d_I}{d_U}$ (WiMAX BS)	99.5	31.4	9.9	3.1	0.99

TABLE I
RELATION BETWEEN SIR_{bit} AND d_I/d_U, FOR $K = 8, \rho = 2.0$.

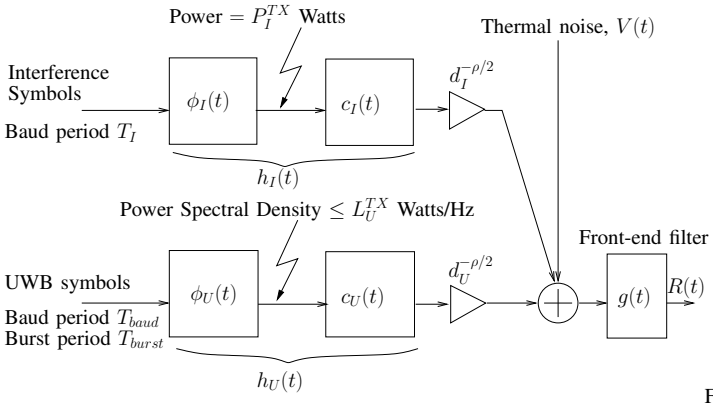

Fig. 1. Signal paths taken by the UWB-IR and the NBI signals.

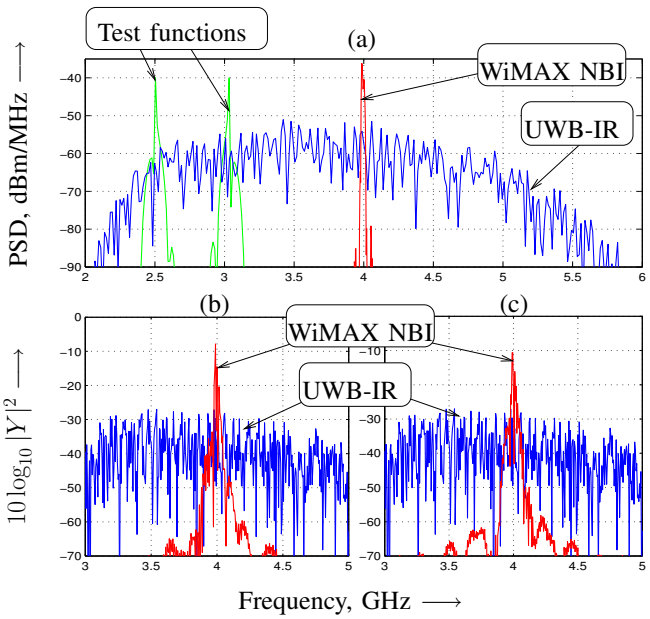

Fig. 2. (a) Received power spectral density of NBI and UWB signals, and the spectra of test functions. (b) and (c) Contribution of UWB and NBI to CS measurements Y, respectively when the NBI falls inbetween two adjacent test functions, and when it is co-located with a test function. $\text{SIR}_{bit} = 20$ dB.

[13] Z. Wang, G. R. Arce, B. M. Sadler, J. L. Paredes, and X. Ma. Compressed Detection for Pilot Assisted Ultra-Wideband Impulse Radio. *IEEE Int. Conf. on UWB*, pages 393–398, September 2007.

[14] R. A. Horn and C. R. Johnson. *Matrix Analysis*. Cambridge University Press, 2005.

[15] S. Boyd and L. Vandenberghe. *Convex Optimization*. Cambridge University Press, 2004.

[16] E. J. Candes, J. Romberg, and T. Tao. Robust Uncertainty Principles: Exact Signal Reconstruction From Highly Incomplete Frequency Information. *IEEE Trans. Inform. Theory*, 52(2):489–509, February 2006.

[17] IEEE Standard for Local and Metropolitan Area Networks Part 16: Air Interface for Fixed Broadband Wireless Access Systems. *IEEE Std 802.16-2004 (Revision of IEEE Std 802.16-2001)*, 2004.

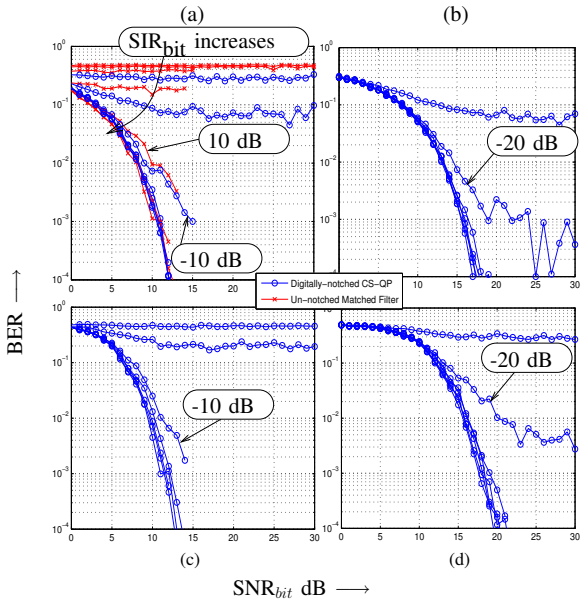

Fig. 3. Effect of WIMAX interference on the BER vs SNR_{bit} performance of a digitally notched CS-QP receiver, for various scenarios of under-sampling and timing uncertainty. (a) Adequate sampling and perfect timing (b) Under-sampling and perfect timing (c) Adequate sampling and poor timing, and (d) Under-sampling and poor timing. In subplot (a) we also show the performance of an un-notched genie-timed matched filter receiver. In each subplot the curves are parametrized by $\text{SIR}_{bit} = -30, -20, -10, 0, 10, 20, \infty$ dB.